Optics & Laser Technology 175 (2024) 110838

Contents lists available at ScienceDirect

Optics and Laser Technology

journal homepage: www.elsevier.com/locate/optlastec

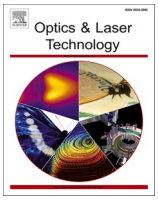

Full length article

LIFT metallization as an alternative to screen-printing for silicon heterojunction solar cells

Cristina Munoz-Garcia [a,*], Ignacio Torres [b,*], David Canteli [a], José Manuel Molla [a], Susana Fernández [b], José Javier Gandía [b], Carlos Molpeceres [a]

[a] Centro Láser-Universidad Politécnica de Madrid, C/ Alan Turing 1, Madrid, Spain
[b] CIEMAT, Renewable Energies Division, Avda. Complutense 40, Madrid, Spain

ARTICLE INFO

Keywords:
Screen-printing
LIFT
Metallization
Heterojunction
Solar cell

ABSTRACT

The electrical characteristics of solar cells are significantly influenced by the metallization process, making it a crucial step. Screen printing is the standard metallization technique, but there is an increasing interest in the development of methods that allow more versatility, higher process control, and a more efficient use of the expensive metallic pastes used. We focus here on the comparison between the standard screen-printing method, and Light-Induced Forward-Transfer (LIFT), a non-contact, very precise technique, able to transfer volumes down to picolitres. The high flexibility, using free-form designs that do not depend on any mask or physical support, and the efficient use of the metallic paste with almost no waste, are other characteristics that point out LIFT as a very promising alternative. In this paper we include the electric characterization of contacts, and solar silicon heterojunction (SHJ) cells metalized with both techniques. The results show a slightly better efficiency for the screen-printed cells, but good series resistance and fill factor values imply that LIFT is a promising alternative for device metallization.

1. Introduction

Monocrystalline silicon cells based on the Pasivated Emmiter Rear Cell (PERC) structure currently dominate the photovoltaic power generation market. However, this technology has certain limitations, including inherent issues such as gap narrowing and Auger recombination losses, as well as challenges related to the structure of the solar cell, such as recombination losses in the contact area. To address these limitations, researchers are continuously searching for more efficient and cost-effective devices. One promising alternative is the use of passivating-contact cells, such as silicon heterojunction (SHJ) cells. In SHJ cells, highly doped p and n contact zones are replaced by a sandwich of intrinsic hydrogenated amorphous silicon (a-Si:H) thin films and doped a-Si:H counterparts. Compared to traditional monocrystalline silicon cells, SHJ cells offer several advantages, including a better temperature coefficient, higher open-circuit voltage, higher conversion efficiency, lower performance degradation, and strong bifacial performance [1,2]. These advantages make SHJ cells a promising candidate for improving the efficiency and reducing the cost of photovoltaic power generation.

But while SHJ is a promising alternative to PERC, it also faces its own challenges. One challenge is that low-temperature processes are necessary when working with SHJ cells. If the cell temperature exceeds 200 °C, hydrogen from the a-Si:H layers is expelled, deteriorating the properties of the a-Si:H thin films and specifically, degrading the passivation of the crystalline silicon surfaces. To mitigate this issue, low-curing temperature pastes are used for the metallization of SHJ cells. However, these types of pastes present a higher electric resistivity than the pastes used in the metallization of other c-Si cells. To address this challenge, pastes with a higher silver concentration (more than 90 %) can be used, as well as using grid electrodes with larger cross-sections. However, this approach increases the cost of device fabrication. In fact, metallization is a limiting step in cell efficiency and a determining factor in the cost of manufacturing SHJ cells. Therefore, reducing the metallization cost is one of the main challenges in the development of SHJ cells. Any advance in a more efficient use of Ag pastes is welcome [2,3], as it can help reduce the cost of manufacturing SHJ cells and improve their competitiveness in the market.

The most common technique for metallizing SHJ cells is screen printing, a reliable, high-productivity technique. Nonetheless, various

* Corresponding authors.
E-mail addresses: cristina.munozg@upm.es (C. Munoz-Garcia), ignacio.torres@ciemat.es (I. Torres).

https://doi.org/10.1016/j.optlastec.2024.110838
Received 15 June 2023; Received in revised form 9 February 2024; Accepted 8 March 2024

metallization techniques are being explored as alternatives to screen printing, with the aim of reducing the consumption of Ag-pastes. These include Pattern Transfer Printing (PTP), which uses lasers to transfer contacts from a polymer tape to the cell surface [4]; Cu electroplating, which involves additional steps of masking and mask-removal [5]; SmartWire Connection Technology (SWCT), which uses copper wires coated with a low melting point alloy [6]; and inkjet printing and FlexTrail printing, which use a voltage-controlled nozzle or a hollow glass capillary to achieve a smaller contact width [7].

One particularly interesting transferring technique is Laser Induced Forward Transfer (LIFT), which involves placing the material to be transferred (the donor layer) onto a transparent substrate (the donor substrate) over the desired substrate (the acceptor substrate), at a fixed distance determined by a spacer. A laser beam is then focused on the interface between the donor layer and donor substrate. By selecting a wavelength that can pass through the transparent substrate and be absorbed by the donor layer, the latter can be partially ejected if a high enough laser fluence is used. A simplified view of the main elements involved in the LIFT process is depicted in Fig. 1.

This straightforward transferring mechanism makes LIFT a powerful and versatile technique that can work with a variety of donor materials, including inks, pastes, and even solid metallic films [8–10]. The versatility of LIFT has led to a wide range of applications, including surface functionalization [11–13], additive manufacturing processes such as the deposition of large aspect ratio pillars, bridges, or more complex designs [14–16], and applications in the field of biomedicine, where the precise control inherent in the process allows for the transfer of single living cells [17–20]. However, perhaps the most direct application is the printing of metallic (and insulating) materials for building electronic circuit elements such as capacitors, resistors, and inductors [21], or as in this study, to deposit the metal grid in a photovoltaic solar cell.

There are several parameters involved in optimizing the LIFT process for printing metallic pastes. These include the viscosity and thickness of the donor film, the laser pulse fluence, the overlap between adjacent laser pulses, the roughness of the acceptor material, and the gap between the donor and acceptor [22–25]. With fast-imaging acquisition techniques, it is possible to observe how the transfer mechanism develops [22,26]. In the case of high-viscosity materials, such as the metallic pastes used in solar cell metallization, the process proceeds as follows: the absorption of the laser radiation at the donor layer/donor substrate interface causes an increase in temperature, leading to the formation of vapor bubbles and the subsequent bulging of the film due to the high pressure generated. As the fluence further increases, the donor film goes from the appearance of the bulge to the breaking or even the explosion of that bulge with the expulsion of material clumps and particles. The right laser pulse fluence and the presence of the acceptor substrate at an adequate distance led to the bulge of metallic paste touching the acceptor and forming a column of paste between donor and acceptor. Finally, when the donor substrate/film is lifted, the column breaks, leaving a paste dot on the acceptor substrate [22,27]. The viscosity of the paste must also be optimized. While a lower density requires a lower pulse fluence for successful transfer, it results in wider voxels and lines. On the other hand, higher densities facilitate the transfer of smaller voxels, but consecutive line deposition becomes impractical [28].

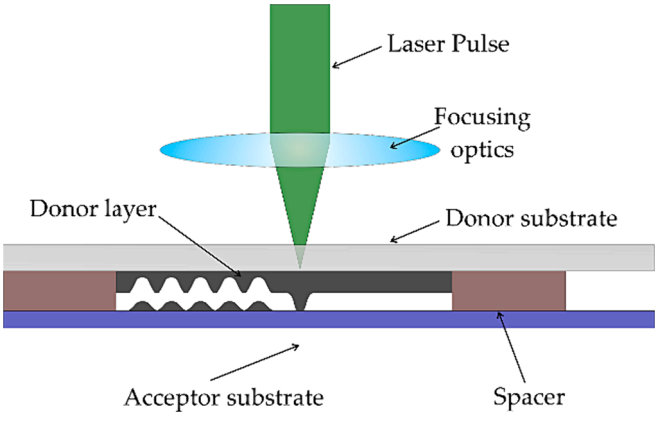

Fig. 1. Schematic description of a LIFT process used to transfer a metallic paste from a donor substrate onto an acceptor.

In this study, we explore LIFT as an alternative method for the metallization of SHJ solar cells. Furthermore, the photovoltaic research community is increasingly interested in validating alternative materials as selective contacts [29], with the aim of reducing the carbon footprint by minimizing high-polluting and energy-demanding deposition processes. Many promising materials, such as 2D materials or organic molecules, require soft post-deposition steps. In this regard, the gentle nature and versatility of LIFT deposition make it an attractive metallization technique beyond its application to SHJ solar cells.

To assess its viability, we present a simple and straightforward comparison between LIFT and screen printing for the metallization of solar cells. Firstly, we focus on parameterizing the LIFT process to obtain metallic lines with suitable electrical and morphological characteristics for the intended application. Next, we compare the electrical characteristics of solar cells metallized by LIFT and screen printing. We conduct the study using SHJ solar cells, a photovoltaic technology that needs to limit any processing step to temperatures below approximately 200 °C, making it a relevant example for other upcoming technologies. Finally, we discuss the advantages and disadvantages of the LIFT process for the specific case of solar cell metallization.

2. Materials and methods

For all the experiments presented, we utilized a commercial silver paste that was specifically produced for the metallization of SHJ cells (Solamet PV416 from DuPont). The paste has a solid content of 81 %—84 % and a viscosity of 90–130 Pa·s according to the product datasheet. It is designed for curing at low temperatures ranging from 130 °C to 180 °C. We conducted tests to measure the electrical resistance of printed lines cured at different temperatures and curing times and observed minimal differences. Therefore, we settled on a curing process of 180 °C for 10 min since SHJ cells also require a final curing step at temperatures of approximately 180 °C to recover the passivation lost after indium-tin-oxide (ITO) deposition [30]. The paste is optimized for screen printing, so it can be used as received for that application. However, viscosity is a critical parameter that needs to be optimized for the LIFT process. Thus, we included a parametrization of the paste viscosity by diluting the as-received product with the recommended thinner (Thinner 8260 from DuPont) in a range of 3 %wt—7%wt for the optimization of the LIFT process.

The LIFT process was carried out as follows: first, the silver paste was spread onto a cleaned glass slide to a thickness of 70 μm using a blade coater (Control Coater model 101 RK from PrintCoat Instruments Ltd.). To control the gap between the donor and acceptor, we affixed a 115 μm-thick polyamide tape (Kapton tape from DuPont) to the donor substrate, creating a gap of approximately 45 μm between the donor layer and the acceptor substrate. As we had prior experience with depositing voxels using similar high-viscosity silver paste [28], our focus was on depositing and curing continuous lines.

The laser system used was a ns-pulsed, Nd:VO_4 DPSS laser source (Explorer from Spectra Physics) that emitted at 532 nm with a full width at half maximum of 15 ns and a maximum power of 2 W (at 50 kHz). The beam waist of the laser system at the focus position was measured to be 18 μm using the ablation threshold method [31]. Finally, the beam was directed to the sample via a galvo scanner with a f-theta lens and focused onto the interface between the donor substrate and silver paste film, ready to transfer the paste.

For the screen-printing process, we used a semi-automatic screen printer (AT-25PA from ATMA) to print different patterns, with lines

widths of approximately 80–100 μm wide. The stainless-steel screens used were provided by Sefar and had a 325-mesh count with a wire diameter of 23 μm and standard mesh angle of $\varphi = 22.5°$.

The morphology of the transferred lines was measured with a confocal microscope (DCM3D, Leica Microsystems). To study its electrical characteristics, lines of different length ranging from 4 mm to 15 mm (see Fig. 2a) were transferred onto ITO-covered glass substrates and the electrical resistance of the lines were measured using a Keithley 2000 multimeter according to the four-point probe method. The resistivity of the transferred lines can then be calculated from:

$$\rho = \frac{R \bullet A}{L} \tag{1}$$

where R is the line's measured resistance, L is the line length, and A is the line cross-section.

In SHJ solar cells, the front metal grid is in direct contact with an ITO layer. Thus, the contact resistivity of the transferred lines with the ITO substrates was also evaluated. The specific contact resistivity was determined by the TLM method [32], using either parallel lines (LIFT, see Fig. 2b top) or parallel contact pads (Screen printing, see Fig. 2b bottom). In the TLM analysis, the measured resistance R_T between two lines or pads of width W and spaced a distance d can be expressed as:

$$R_T = \frac{R_{sh}(d + 2L_T)}{W} \tag{2}$$

with R_{sh} being the sheet resistance of the ITO substrate, and L_T the transfer length. Thus, by measuring R_T for different d values, R_{sh} and L_T can be obtained, and the specific contact resistivity (ρ_c) can be calculated as:

$$\rho_c = R_{sh} {L_T}^2. \tag{3}$$

Following the optimization of the LIFT process for transferring the conductive silver paste, SHJ solar cells (see Fig. 3) were fabricated were the front metal grid was deposited by either LIFT or screen-printing. The solar cells were fabricated using 280 μm-thick double-side polished n-type c-Si wafers ⟨100⟩ with a resistivity of 1–3 Ω·cm. The different amorphous silicon thin films were deposited in a two-chamber plasma-enhanced chemical vapor deposition (PECVD) commercial reactor (Electtrorava s.p.a.) following the sequence found in [33]. The back contact consisted on a full-area Ag electrode deposited in a thermal evaporation system (Univex300, Leybold GmbH). Lastly, the front side was covered with an 80 nm thick ITO layer sputtered at room temperature using an Ar atmosphere from a In_2O_3:SnO_2 (90/10 wt%) ceramic target powered by DC (Univex 450B, Leybold). For the metallization of the front contact, we used a design consisting in a solid frame 0.85 mm wide, leaving a cell area of 1 cm^2 with five parallel fingers, 100 μm wide, regularly spaced with a pitch of 1.67 mm to extract the electric current (see Fig. 2c).

The current density–voltage (JV) characteristics of the devices were measured under illumination, calibrated at AM1.5G conditions and 100 mW/cm^2, using a class A solar simulator (Steuernagel SC575). Additionally, Suns-V_{oc} measurements were performed (WCT-120, Sinton Instrument) to evaluate the series resistance (R_s) as detailed in [34].

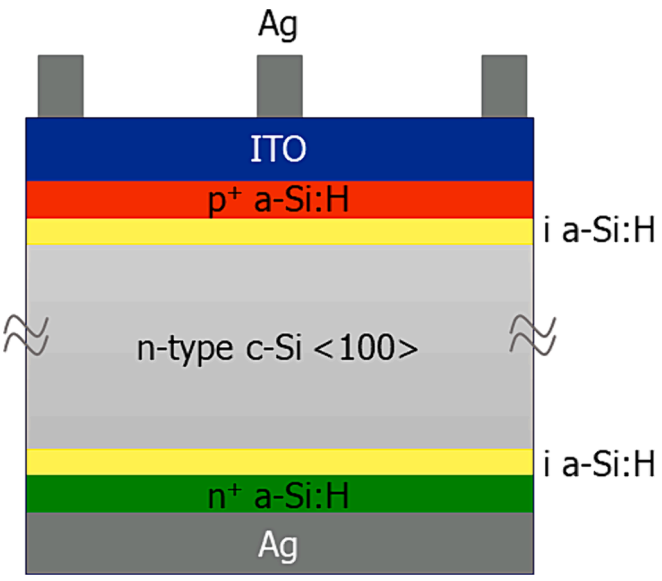

Fig. 3. Structure of a silicon heterojunction (SHJ) solar cell.

3. Results

3.1. Morphology optimization of transferred lines

To make an objective comparison regarding the performance of the transferred lines obtained by the two techniques, the aim with the LIFT process was to achieve lines approximately 100 μm wide, similar to the screen-printed results. In our first attempt, we tried to transfer lines by using the as-received paste (no further dilution) and employing pulse energies (E_p) ranging between 10.5 μJ and 27 μJ while keeping pulse frequency at 20 KHz and the scanner speed at 1 m/s. Even at the highest energies employed we could not observe any material transferred onto the acceptor, indicating that possibly the viscosity of the paste was excessively high for the set-up used.

Therefore, the next step was to study the effect of diluting down the paste by pre-mixing it with a controlled percentage of thinner. We prepared different dilutions, spanning from a 4 % weight dilution up to a 7 %, and performed several LIFT processes by varying E_p from 10.5 μJ and 27 μJ. Regarding the lines' width achieved, Fig. 4a shows the measured values as a function of E_p at different dilution percentage using a glass substrate. For a given dilution percentage there is an E_p threshold below which no paste is transferred (indicated by the lines prior the first data points in Fig. 4). Above that threshold, as E_p increases, each pulse transfers a higher amount of paste, and wider lines are obtained.

Likewise, the effect of the dilution percentage is that wider lines are obtained as higher dilutions are used. On the one hand, a more diluted paste has a lower energy threshold for the LIFT process (more diluted

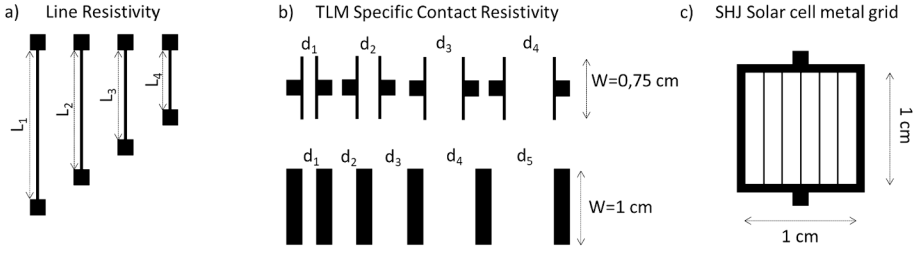

Fig. 2. Different patterns transferred using the LIFT technique and screen-printing for the characterization of the line resistivity (a) and the specific contact resistivity using the TLM analysis (b); and for the metallization of the SHJ solar cells (c).

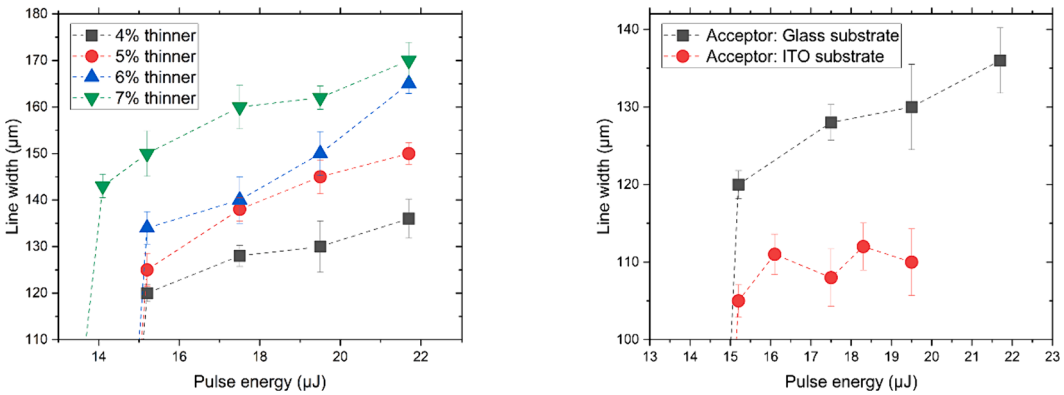

Fig. 4. (**a**) Width of lines deposited by LIFT onto a glass substrate as function of laser pulse energy, for different percentages of thinner. (b) Effect of using different acceptor substrate (Glass or ITO) for lines transferred at different pulse energies (thinner 4 %). Laser repetition frequency (20 kHz), process speed (1 m/s), donor film thickness (70 μm) and gap between donor and acceptor (45 μm) remained fixed in (a) and (b). The width value and the error bars represent the average and the deviation of five different measurements taken along the length of the lines.

pastes can be transferred at lower Ep as observed in prior studies [30]). On the other hand, transferred pastes with lower viscosity spread more easily as they reach the acceptor substrate, explaining the observed results. With a weight dilution of a 4 % and a pulse energy of 15.15 μJ, we obtained a transferred lines' width of 120 μm.

None of the lines completed achieved the objective of a 100 μm width. However, the paste used is specifically designed to provide a good adhesion to ITO substrates. By changing the acceptor from glass to ITO, the better adhesion reduces droplet spreading and the width of the lines is significantly reduced as shown in Fig. 4b, where we show line widths closer to 100 μm. Since with ITO the spreading of the droplets as they hit the acceptor substrate is reduced, the effect of E_p is also diminished and the variation in width is significantly reduced. For this reason, for subsequent experiments we fixed E_p at 19.5 μJ since the widths obtained were only marginally larger compared to lower E_p values and we observed a better homogeneity along the transferred lines together with improved reproducibility between experiments.

With increased adhesion, we also observed a more irregular transferred lines (see left image in Fig. 5) with regions where just one of each two pulses transferred material. We ascribe this effect to an excessive overlap: when adjacent pulses are too close the gas bubble generated by a pulse can be connected to the cavity produced by the previous one, leading to no paste transfer. This effect on the interaction between adjacent pulses leading to transfer failures has been previously reported by several authors [35,36]. It is therefore necessary to adopt a larger spot pitch to avoid interactions and ensure a successful transfer [37].In this work, by doubling the speed of the process and increasing the spot pitch we obtained continuous lines with a smooth morphology and widths of 105–110 μm and 0.21 aspect ratio [see Fig. 5 right], reaching the proposed objective.

3.2. *Electrical properties of the transferred lines and contact resistance*

Using the pattern shown in Fig. 2a, we transferred silver paste lines by LIFT with the optimized lasing parameters (f = 20 kHz, v = 2 m/s, Ep = 19.5 μJ and a 4 % dilution) as well as by screen-printing. As can be seen in Fig. 6, the lines obtained by both techniques exhibit a uniform appearance although printed lines are slightly narrower and lower than LIFT transferred lines (aspect ratio for LIFT lines is ~ 0.2 compared to ~ 0.15).

Fig. 7 shows the measured resistance (after sintering at 180 ℃) as a function of the line length. For both techniques, the resistivity calculated

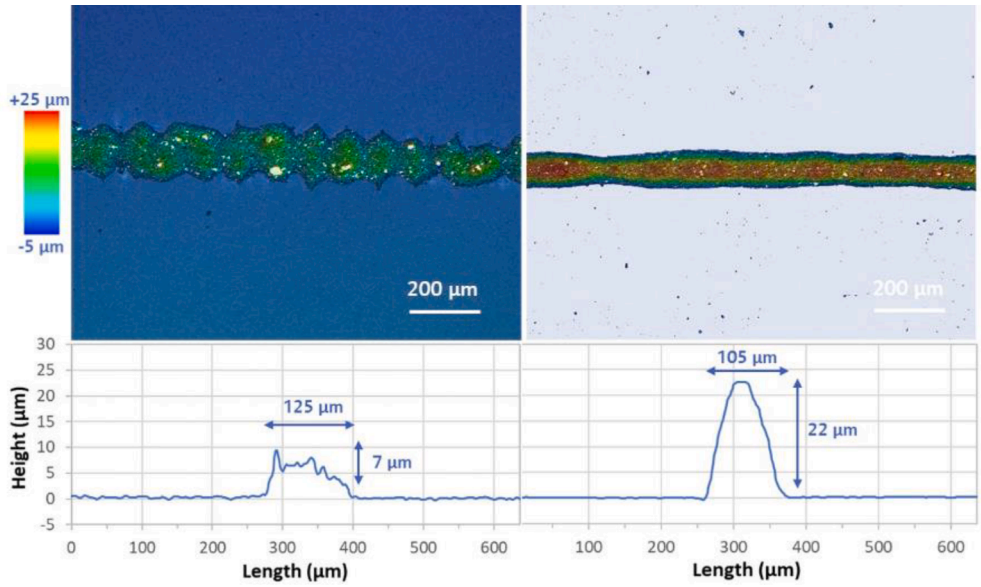

Fig. 5. Lines of 4 % diluted paste transferred at a repetition pulse frequency of 20 kHz, with a pulse energy of 19.5 μJ over ITO at 1000 mm/s (left) and 2000 mm/s (right).

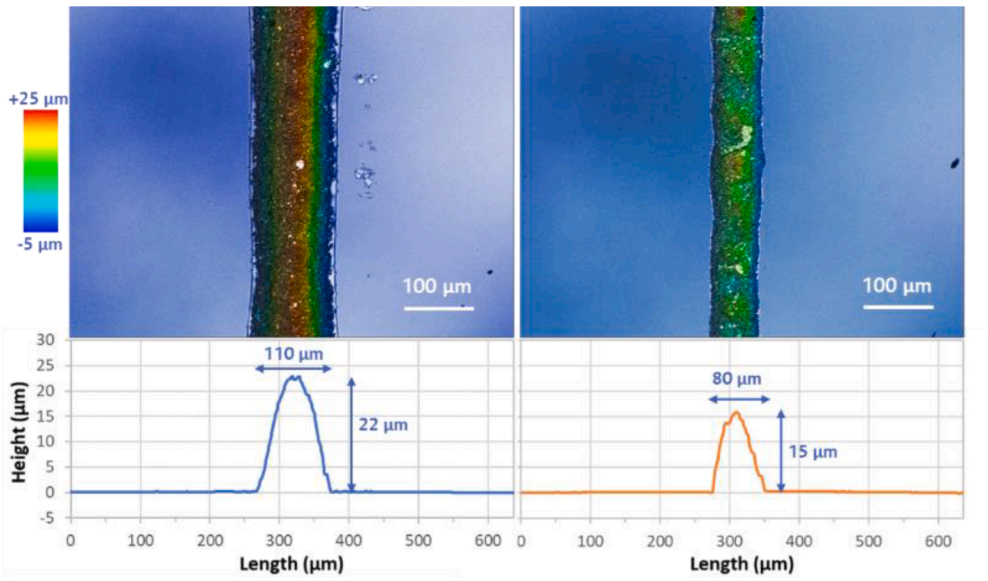

Fig. 6. Lines used for the electric characterization of silver paste lines, obtained by LIFT (left) and screen-printing (right).

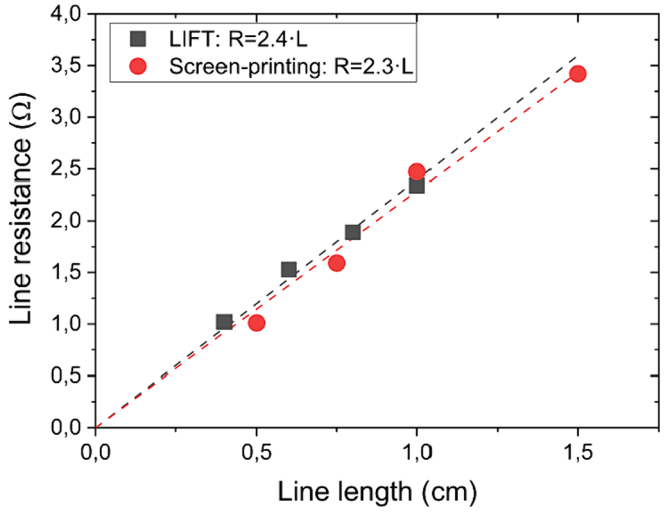

Fig. 7. Line resistance measured as a function of line length for both LIFT and screen-printing and fit used to calculate the resistivity from equation (1).

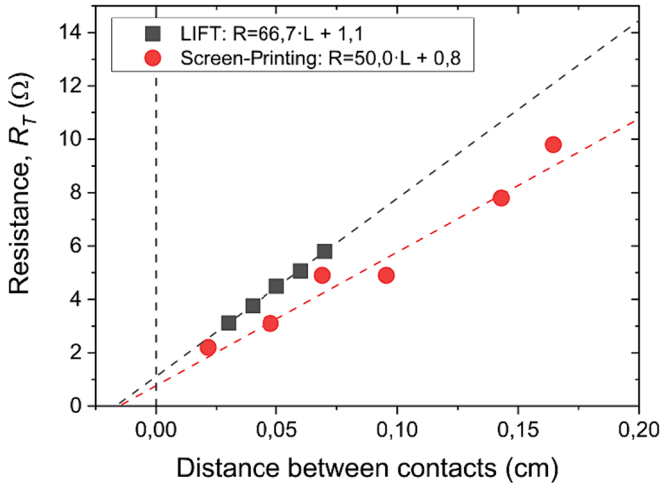

Fig. 8. TLM measurements obtain for Ag transferred contacts onto an ITO substrate.

using equation (1) is ~ 20 µΩ·cm for the screen-printed lines and ~ 40 µΩ·cm for the lines deposited by LIFT. The reason why the lines deposited by LIFT showed a higher resistivity is unclear but could be related to a combination of i) a reduction in the metal loading per unit area in thinned down pastes; and ii) larger inhomogeneity in the lines' cross sections (compared to screen printed lines) leading to an over estimation in the resistivity. Nevertheless, both values are less than a factor of ten lower than typical values obtained for printed silver lines sintered at much higher temperatures [38] and only one order of magnitude lower than bulk silver (~1.6 µΩ·cm).

Next, we measured the specific contact resistance of the deposited silver paste with the ITO substrate using the patterns shown in Fig. 2b for LIFT (top image) and screen-printing (bottom image). The measured resistance as a function of the distance between the contacts is plotted in Fig. 8, and the values obtained from the fitting of the data to equations (2) and (3) are collected in Table 1.

The results obtained for both methods are again very similar (note that the differences in the slopes in Fig. 8 are due to the differences in contact length, *W*). The extracted sheet resistance for the ITO substrate is the same with either sample (and correct as checked with a four-point probe system), validating the experimental data. And since there are minimal differences in the transfer length, the specific contact resistance is also comparable, and both below the target value of 5 mΩ·cm^2 deemed acceptable for silicon heterojunction technology [38].

Table 1
Values calculated from the TLM measurements (see Fig. 8).

Parameter	LIFT	Screen-printing
Contact Length, *W* [mm]	7.5	10.0
Transfer length, L_T [mm]	0.0083	0.0078
Sheet resistance, R_{sh} [Ω/□]	50.03	50.02
Specific contact resistivity, ρ_c [mΩ·cm^2]	3.45	3.04

3.3. Heterojunction silicon solar cells performance

To conclude the comparison study, we completed the front grid metallization of four different SHJ solar cells with LIFT and screen-printing according to the design in Fig. 2c. The measured JV

characteristics under illumination of the four different cells are plotted in Fig. 9 and the extracted parameters for the best performing cells are listed in Table 2.

As can be seen from Table 2, both techniques delivered cells achieving a very similar performance. Since the solar cells used for this study were not textured, the maximum efficiency is limited by the low short circuit current (J_{sc}). The metallization step is expected to have the biggest impact to the fill-factor (*FF*) since it is directly affected by resistive losses, and to J_{sc} due to shadowing effects. The open-circuit voltage (V_{oc}) is mostly governed by the quality of the junction and thus the metallization process has limited impact unless the curing temperature is above the amorphous silicon films processing temperature.

The values of *FF* measured for both metallization techniques were the same (74 % for the best performing cells and 71 % for the other two cells). The values of J_{sc} were lower for the two cells with the contacts transferred by LIFT as seen in Fig. 8, with the differences observed being consistent with the finger widths achieved (around 110 μm for LIFT contacts and 80 μm for screen-printed ones). In accordance with the values of the specific contact resistivity shown in subsection 3.2, the R_s values calculated according to [34] using the Suns-V_{oc} method were slightly smaller for the screen-printed cells, but hardly a significant difference (see Table 2 and the differences in slope of the *JV* curves at high forward voltages).

Ultimately, these results suggest that LIFT is a valid metallization technique, comparable to screen-printing in terms of solar-cell performance. Furthermore, LIFT has some inherent qualities that makes it a very interesting metallization option worth investigating. On the one hand, LIFT is much more flexible than screen-printing, allowing any pattern to be printed almost on the go, without the need for masks. In addition, the use of the silver paste can be further optimize with the LIFT technique, minimizing silver-paste wastage often observed in screen-printing. On the other hand, screen-printing is still more suited for a production-level metallization process, giving it a great advantage over LIFT in the industrial setting. Nevertheless, there are many examples of applications that have implemented LIFT at an industrial level, such as printing OLED pixels in high-end televisions [39] or chip bonding and assembly in the microelectronics industry [40]. But, LIFT microfabrication is not limited to 2D structures only, 3D structures can be made repeating the laser transfer process of individual voxels at the same location [15]. In recent years, interest in using LIFT techniques for different materials has increased, the main applications being microelectronics, flexible electronics and photovoltaics. In conclusion, we have before us a new innovative technique that will allow its industrial integration in different strategic sectors once it reaches its highest point of maturity [41].

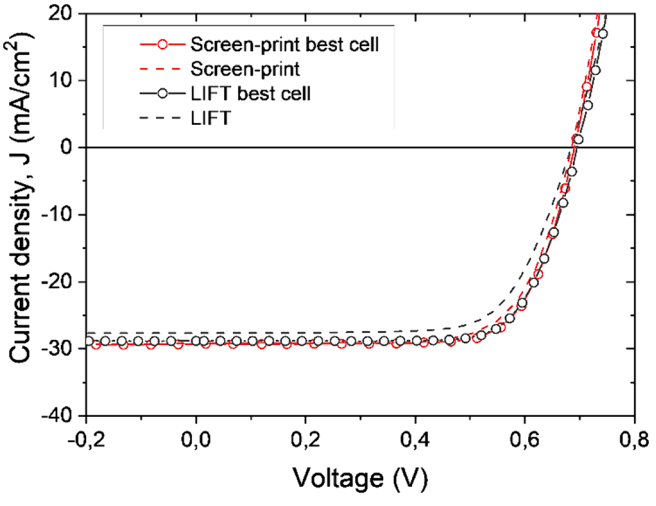

Fig. 9. JV characteristics of the four SHJ cells metalized by LIFT (black curves) and screen-printing (red curves) measured under AM1.5G irradiation.

Table 2
Solar cells characteristic parameters for the best fabricated cells using LIFT and scree-printing for the metallization of the front grid. The JV curves of the best cells are represented in Fig. 9.

Parameter	LIFT, best cell	Screen-printing, best cell
Short-circuit current density, J_{SC} (mA/cm^2)	28.82	29.28
Open-circuit voltage, V_{OC} (mV)	695	690
Current density at MPP, J_{mp} (mA/cm^2)	27.05	26.82
Voltage at MPP, V_{mp} (mV)	547	556
Fill factor, *FF (%)*	74	74
Efficiency, η (%)	14.8	14.9
Series resistance, R_S (Ω·cm^2)	2.36	2.16

Therefore, with enough effort and research geared towards this particular application, both in terms of the silver-paste composition and the LIFT process, it could end up challenging screen-printing as the de facto technique for the metallization of solar cells.

4. Conclusions

We have presented a comparison between LIFT and screen-printing as the metallization method for silicon heterojunction (SHJ) solar cells, using a commercial silver paste specifically designed for this solar cell technology. By adjusting the laser power and the rheology of the silver paste (adding a thinning agent), we could systematically transfer silver lines 110 μm wide when using ITO as the acceptor substrate, while the screen-printed lines were 80–100 μm wide. After curing the lines at 180 °C, the measured line resistivity for both techniques was in the order of 20 μΩ·cm for the screen-printed lines and 40 μΩ·cm for the lines deposited by LIFT, both values suitable for the studied application. Regarding the specific contact resistivity between mΩ the silver paste transferred and the ITO substrate, both techniques achieved similar results, with LIFT obtaining a slightly larger value (3.45 mΩ·cm^2 vs 3.04 mΩ·cm^2). Once again, both values are well below the minimum required target of 5 ·cm^2 for SHJ technology. Finally, SHJ cells metallized with both technologies showed comparable performances, especially regarding the fill factor achieved, a parameter that is directly affected to any resistive losses that may incur due to a faulty metallization. The solar cell metallized using LIFT had a slightly lower short-circuit current as a result of the slightly wider contact fingers. In conclusion, we have shown that the LIFT technique is suitable for the fabrication of SHJ solar cells and that with enough research towards this particular process, it could end up being a viable industrial alternative to screen-printing with added flexibility and reduced silver consumption.

CRediT authorship contribution statement

Cristina Munoz-Garcia: Investigation, Methodology, Writing – original draft, Writing – review & editing. **Ignacio Torres:** Conceptualization, Investigation, Methodology, Writing – original draft, Writing – review & editing. **David Canteli:** Investigation, Methodology, Writing – original draft, Writing – review & editing. **José Manuel Molla:** Investigation, Methodology. **Susana Fernández:** Writing – review & editing. **José Javier Gandía:** Funding acquisition, Writing – review & editing. **Carlos Molpeceres:** Conceptualization, Funding acquisition, Supervision, Writing – review & editing.

Declaration of competing interest

The authors declare that they have no known competing financial interests or personal relationships that could have appeared to influence the work reported in this paper.

Data availability

Data will be made available on request.

Acknowledgments

Partial financial support has been provided by the Spanish Ministry of Science and Innovation under the project SCALED (PID2019–109215RB-C42 and PID2019–109215RB-C44).

References

[1] Y. Liu, Y. Li, Y. Wu, G. Yang, L. Mazzarella, P. Procel-Moya, A.C. Tamboli, K. Weber, M. Boccard, O. Isabella, X. Yang, B. Sun, High-efficiency silicon heterojunction solar cells: Materials, devices and applications, Mater. Sci. Eng. R Reports. 142 (2020), https://doi.org/10.1016/j.mser.2020.100579.
[2] S. DeWolf, A. Descoeudres, Z.C. Holman, C. Ballif, High-efficiency silicon heterojunction solar cells: A review, Green. 2 (2012) 7–24, https://doi.org/10.1515/green-2011-0018.
[3] M. Taguchi, A. Yano, S. Tohoda, K. Matsuyama, Y. Nakamura, T. Nishiwaki, K. Fujita, E. Maruyama, 24.7% record efficiency HIT solar cell on thin silicon wafer, IEEE J. Photovoltaics. 4 (2014) 96–99, https://doi.org/10.1109/JPHOTOV.2013.2282737.
[4] J. Lossen, M. Matusovsky, A. Noy, C. Maier, M. Bähr, Pattern transfer printing (PTPTM) for c-Si solar cell metallization, Energy Procedia 67 (2015) 156–162, https://doi.org/10.1016/j.egypro.2015.03.299.
[5] Z. Li, P.C. Hsiao, W. Zhang, R. Chen, Y. Yao, P. Papet, A. Lennon, Patterning for plated heterojunction cells, Energy Procedia 67 (2015) 76–83, https://doi.org/10.1016/j.egypro.2015.03.290.
[6] P. Papet, L. Andreetta, D. Lachenal, G. Wahli, J. Meixenberger, B. Legradic, W. Frammelsberger, D. Bätzner, B. Strahm, Y. Yao, T. Söderström, New cell metallization patterns for heterojunction solar cells interconnected by the smart wire connection technology, Energy Procedia 67 (2015) 203–209, https://doi.org/10.1016/j.egypro.2015.03.039.
[7] J. Schube, T. Fellmeth, M. Jahn, R. Keding, S.W. Glunz, Advanced metallization with low silver consumption for silicon heterojunction solar cells, AIP Conference Proceedings 2156 (2019), https://doi.org/10.1063/1.5125872.
[8] I. Zergioti, Laser printing of organic electronics and sensors, J. Laser Micro Nanoeng. 8 (2013) 30–34, https://doi.org/10.2961/jlmn.2013.01.0007.
[9] E. Breckenfeld, H. Kim, R.C.Y. Auyeung, N. Charipar, P. Serra, A. Piqué, Laser-induced forward transfer of silver nanopaste for microwave interconnects, Appl. Surf. Sci. 331 (2015) 254–261, https://doi.org/10.1016/j.apsusc.2015.01.079.
[10] J.A. Grant-Jacob, B. Mills, M. Feinaeugle, C.L. Sones, G. Oosterhuis, M. B. Hoppenbrouwers, R.W. Eason, Micron-scale copper wires printed using femtosecond laser-induced forward transfer with automated donor replenishment, Opt. Mater. Express. 3 (2013) 747, https://doi.org/10.1364/ome.3.000747.
[11] H.-J. Li, W.-Z. Fan, H.-H. Pan, C.-W. Wang, J. Qian, Q.-Z. Zhao, Fabrication of "petal effect" surfaces by femtosecond laser-induced forward transfer, Chem. Phys. Lett. 667 (2017) 20–24, https://doi.org/10.1016/j.cplett.2016.11.026.
[12] M.L. Tseng, C.M. Chang, B.H. Chen, Y.-W. Huang, C.H. Chu, K.S. Chung, Y.J. Liu, H.G. Tsai, N.-N. Chu, D.-W. Huang, H.-P. Chiang, D.P. Tsai, Fabrication of plasmonic devices using femtosecond laser-induced forward transfer technique, Nanotechnol. 23 (2012) 444013, https://doi.org/10.1088/0957-4484/23/44/444013.
[13] P. Delaporte, A.-P. Alloncle, Laser-induced forward transfer: A high resolution additive manufacturing technology, Opt. Laser Technol. 78 (2016) 33–41, https://doi.org/10.1016/j.optlastec.2015.09.022.
[14] M. Zenou, Z. Kotler, Printing of metallic 3D micro-objects by laser induced forward transfer, Opt. Express. 24 (2016) 1431, https://doi.org/10.1364/oe.24.001431.
[15] A. Piqué, R.C.Y.Y. Auyeung, H. Kim, N.A. Charipar, S.A. Mathews, Laser 3D micro-manufacturing, J. Phys. d. Appl. Phys. 49 (2016) 223001, https://doi.org/10.1088/0022-3727/49/22/223001.
[16] D.J. Heath, M. Feinaeugle, J.A. Grant-Jacob, B. Mills, R.W. Eason, Dynamic spatial pulse shaping via a digital micromirror device for patterned laser-induced forward transfer of solid polymer films, Opt. Mater. Express. 5 (2015) 1129, https://doi.org/10.1364/ome.5.001129.
[17] C.Y. Chen, J.A. Barron, B.R. Ringeisen, Cell patterning without chemical surface modification: Cell-cell interactions between printed bovine aortic endothelial cells (BAEC) on a homogeneous cell-adherent hydrogel, Appl. Surf. Sci. 252 (2006) 8641–8645, https://doi.org/10.1016/j.apsusc.2005.11.088.
[18] M. Gruene, M. Pflaum, A. Deiwick, L. Koch, S. Schlie, C. Unger, M. Wilhelmi, A. Haverich, B.N. Chichkov, Adipogenic differentiation of laser-printed 3D tissue grafts consisting of human adipose-derived stem cells, Biofabrication 3 (2011), https://doi.org/10.1088/1758-5082/3/1/015005.
[19] A. Marquez, M. Gómez-Fontela, S. Lauzurica, R. Candorcio-Simón, D. Munoz-Martin, M. Morales, M. Ubago, C. Toledo, P. Lauzurica, C. Molpeceres, Fluorescence enhanced BA-LIFT for single cell detection and isolation, Biofabrication 12 (2020) 025019, https://doi.org/10.1088/1758-5090/ab6138.
[20] R. Xiong, Z. Zhang, W. Chai, Y. Huang, D.B. Chrisey, Freeform drop-on-demand laser printing of 3D alginate and cellular constructs, Biofabrication 7 (2015) 45011, https://doi.org/10.1088/1758-5090/7/4/045011.
[21] A. Piqué, D.B. Chrisey, R.C.Y. Auyeung, J. Fitz-Gerald, H.D. Wu, R.A. McGill, S. Lakeou, P.K. Wu, V. Nguyen, M. Duignan, A novel laser transfer process for direct writing of electronic and sensor materials, Appl. Phys. A Mater. Sci. Process. 69 (1999) S279–S284, https://doi.org/10.1007/s003390051400.
[22] D. Munoz-Martin, C.F. Brasz, Y. Chen, M. Morales, C.B. Arnold, C. Molpeceres, Laser-induced forward transfer of high-viscosity silver pastes, Appl. Surf. Sci. 366 (2016) 389–396, https://doi.org/10.1016/j.apsusc.2016.01.029.
[23] E. Turkoz, M. Morales, S.Y. Kang, A. Perazzo, H.A. Stone, C. Molpeceres, C. B. Arnold, Laser-induced forward transfer from healing silver paste films, Appl. Phys. Lett. 113 (2018), https://doi.org/10.1063/1.5060717.
[24] Y. Chen, M. Morales, D. Munoz-Martin, C. Molpeceres, Influence of the acceptor roughness on the aspect ratio of silver paste lines printed by laser-induced forward transfer, Results Phys. 6 (2016) 998–999, https://doi.org/10.1016/j.rinp.2016.11.015.
[25] D. Munoz-martin, Y. Chen, M. Morales, C. Molpeceres, Overlapping limitations for ps-pulsed lift printing of high viscosity metallic pastes, Metals (basel). 10 (2020), https://doi.org/10.3390/met10020168.
[26] J. Moreno-Labella, D. Munoz-Martin, A. Márquez, M. Morales, C. Molpeceres, Numerical study of water-glycerol BA-LIFT: Analysis and simulation of secondary effects, Opt. Laser Technol. 135 (2021) 106695, https://doi.org/10.1016/j.optlastec.2020.106695.
[27] M. Duocastella, J.M. Fernández-Pradas, J.L. Morenza, P. Serra, Time-resolved imaging of the laser forward transfer of liquids, J. Appl. Phys. 106 (2009) 084907, https://doi.org/10.1063/1.3248304.
[28] D. Canteli, D. Munoz-Martin, M. Morales, S. Lauzurica, J.J. Moreno, A. Márquez, M. Gómez-Fontela, C. Molpeceres, Laser-Induced Forward Transfer of silver-based pastes for metallization of photovoltaic devices, in: G. Račiukaitis, T. Makimura, C. Molpeceres (Eds.), Laser Appl. Microelectron. Optoelectron. Manuf. XXIV, SPIE, 2019 21 10.1117/12.2508975.
[29] L.G. Gerling, S. Mahato, A. Morales-Vilches, G. Masmitja, P. Ortega, C. Voz, R. Alcubilla, J. Puigdollers, Transition metal oxides as hole-selective contacts in silicon heterojunctions solar cells, Sol. Energy Mater. Sol. Cells. 145 (2016) 109–115, https://doi.org/10.1016/j.solmat.2015.08.028.
[30] B. Demaurex, S. De Wolf, A. Descoeudres, Z. Charles Holman, C. Ballif, Damage at hydrogenated amorphous/crystalline silicon interfaces by indium tin oxide overlayer sputtering, Appl. Phys. Lett. 101 (2012) 171604, https://doi.org/10.1063/1.4764529.
[31] J.M. Liu, Simple technique for measurements of pulsed gaussian-beam spot sizes, Opt. Lett. 7 (1982) 196, https://doi.org/10.1364/OL.7.000196.
[32] S. Guo, G. Gregory, A.M. Gabor, W.V. Schoenfeld, K.O. Davis, Detailed investigation of TLM contact resistance measurements on crystalline silicon solar cells, Sol. Energy. 151 (2017) 163–172, https://doi.org/10.1016/j.solener.2017.05.015.
[33] I. Torres, S. Fernández, M. Fernández-Vallejo, I. Arnedo, J.J. Gandía, Graphene-based electrodes for silicon heterojunction solar cell technology, Mater. (basel). 14 (2021) 4833, https://doi.org/10.3390/ma14174833.
[34] D. Pysch, A. Mette, S.W. Glunz, A review and comparison of different methods to determine the series resistance of solar cells, Sol. Energy Mater. Sol. Cells. 91 (2007) 1698–1706, https://doi.org/10.1016/j.solmat.2007.05.026.
[35] P. Sopeña, J.M. Fernández-Pradas, P. Serra, Laser-induced forward transfer of conductive screen-printing inks, Appl. Surf. Sci. 507 (2020) 145047, https://doi.org/10.1016/j.apsusc.2019.145047.
[36] Y. Chen, D. Munoz-Martin, M. Morales, C. Molpeceres, E. Sánchez-Cortezon, J. Murillo-Gutierrez, Laser induced forward transfer of high viscosity silver paste for new metallization methods in photovoltaic and flexible electronics industry, Phys. Procedia. 83 (2016) 204–210, https://doi.org/10.1016/j.phpro.2016.08.010.
[37] Y. Shan, X. Zhang, H. Li, Z. Zhan, Single-step printing of high-resolution, high-aspect ratio silver lines through laser-induced forward transfer, Opt. Laser Technol. 133 (2021) 106514, https://doi.org/10.1016/j.optlastec.2020.106514.
[38] J. Schube, L. Tutsch, T. Fellmeth, M. Bivour, F. Feldmann, T. Hatt, F. Maier, R. Keding, F. Clement, S.W. Glunz, Low-resistivity screen-printed contacts on indium tin oxide layers for silicon solar cells with passivating contacts, IEEE J. Photovoltaics. 8 (2018) 1208–1214, https://doi.org/10.1109/JPHOTOV.2018.2859768.
[39] J. Shaw Stewart, T. Lippert, M. Nagel, F. Nüesch, A. Wokaun, Red-green-blue polymer light-emitting diode pixels printed by optimized laser-induced forward transfer, Appl. Phys. Lett. 100 (2012) 203303, https://doi.org/10.1063/1.4717463.
[40] F. Zacharatos, M. Makrygianni, I. Zergioti, Laser-induced forward transfer (LIFT) technique as an alternative for assembly and packaging of electronic components, IEEE J. Sel. Top. Quantum Electron. 27 (2021) 1–8, https://doi.org/10.1109/JSTQE.2021.3084443.
[41] M. Morales, D. Munoz-Martin, A. Marquez, S. Lauzurica, C. Molpeceres, Laser-induced forward transfer techniques and applications, second edi, Elsevier Ltd. (2018), https://doi.org/10.1016/b978-0-08-101252-9.00013-3.